Publication Year	2016
Acceptance in OA@INAF	2020-05-27T14:04:13Z
Title	Modeling pyramidal sensors in ray-tracing software by a suitable user-defined surface
Authors	Antichi, Jacopo; MUNARI, MATTEO; MAGRIN, DEMETRIO; RICCARDI, Armando
DOI	10.1117/1.JATIS.2.2.028001
Handle	http://hdl.handle.net/20.500.12386/25240
Journal	JOURNAL OF ASTRONOMICAL TELESCOPES, INSTRUMENTS, AND SYSTEMS
Number	2

Journal of Astronomical Telescopes, Instruments, and Systems

AstronomicalTelescopes.SPIEDigitalLibrary.org

Modeling pyramidal sensors in ray-tracing software by a suitable user-defined surface

Jacopo Antichi
Matteo Munari
Demetrio Magrin
Armando Riccardi

SPIE.

Jacopo Antichi, Matteo Munari, Demetrio Magrin, Armando Riccardi, "Modeling pyramidal sensors in ray-tracing software by a suitable user-defined surface," *J. Astron. Telesc. Instrum. Syst.* **2**(2), 028001 (2016), doi: 10.1117/1.JATIS.2.2.028001.

Downloaded From: https://www.spiedigitallibrary.org/journals/Journal-of-Astronomical-Telescopes,-Instruments,-and-Systems on 14 Apr 2021
Terms of Use: https://www.spiedigitallibrary.org/terms-of-use

Modeling pyramidal sensors in ray-tracing software by a suitable user-defined surface

Jacopo Antichi,[a,*] Matteo Munari,[b] Demetrio Magrin,[c] and Armando Riccardi[a]
[a]Istituto Nazionale di Astrofisica-Osservatorio Astrofisico di Arcetri, Largo Enrico Fermi 5, 50125 Firenze, Italy
[b]Istituto Nazionale di Astrofisica-Osservatorio Astrofisico di Catania, Via Santa Sofia, 95123 Catania, Italy
[c]Istituto Nazionale di Astrofisica-Osservatorio Astronomico di Padova, Via Vicolo Osservatorio 5, 35100 Padova, Italy

Abstract. Following the unprecedented results in terms of performances delivered by the first light adaptive optics system at the Large Binocular Telescope, there has been a wide-spread and increasing interest on the pyramid wavefront sensor (PWFS), which is the key component, together with the adaptive secondary mirror, of the adaptive optics (AO) module. Currently, there is no straightforward way to model a PWFS in standard sequential ray-tracing software. Common modeling strategies tend to be user-specific and, in general, are unsatisfactory for general applications. To address this problem, we have developed an approach to PWFS modeling based on user-defined surface (UDS), whose properties reside in a specific code written in C language, for the ray-tracing software ZEMAX™. With our approach, the pyramid optical component is implemented as a standard surface in ZEMAX™, exploiting its dynamic link library (DLL) conversion then greatly simplifying ray tracing and analysis. We have utilized the pyramid UDS DLL surface—referred to as pyramidal acronyms may be too risky (PAM2R)—in order to design the current PWFS-based AO system for the Giant Magellan Telescope, evaluating tolerances, with particular attention to the angular sensitivities, by means of sequential ray-tracing tools only, thus verifying PAM2R reliability and robustness. This work indicates that PAM2R makes the design of PWFS as simple as that of other optical standard components. This is particularly suitable with the advent of the extremely large telescopes era for which complexity is definitely one of the main challenges. © *2016 Society of Photo-Optical Instrumentation Engineers (SPIE)* [DOI: 10.1117/1.JATIS.2.2.028001]

Keywords: adaptive optics; wavefront sensor; ray tracing; surface modeling.

Paper 15083 received Dec. 16, 2015; accepted for publication Apr. 27, 2016; published online May 27, 2016.

1 Introduction

Modeling pyramid wavefront sensors (PWFSs) is complicated in sequential ray-tracing software due to the geometry of its main optical component: the pyramid. For wavefront sensing purposes, typically the vertex of a four surfaces' refractive pyramid is located in a focal plane as introduced for the first time by Ragazzoni.[1] It can also consist of a double (or even multiple) refractive pyramid, as presented by Diolaiti et al.[2] and Tozzi et al.,[3] with the second pyramidal surfaces introduced mainly in order to simplify the pyramid manufacturability and to reduce chromatic effects in broad band applications. Moreover, it can also consist of a reflective pyramidal surface as proposed by Wang et al.[4] Despite being 20 years from its first application in a single-conjugated adaptive optics (AO) mode at Telescopio Nazionale Galileo[5] and 10 years from its first application into a multiconjugated AO mode at the Very Large Telescope[6] (VLT), only recently have the advantages of PWFS been largely accepted by the AO community thanks to the unprecedented results obtained by the first light adaptive optics (FLAO).[7] In synthesis, through the efforts of more than a generation of astronomers working on this subject at the Large Binocular Telescope, PWFS operates nowadays on big AO facilities far from Arizona, e.g., MagAO[8] and SCExAO,[9] and it has been proposed for a third generation VLT instrument as well.[10]

The properties of this sensor in terms of dynamic range, sensitivity, and linearity have been the subject of decadal research in optics, and they have been resumed by Guyon[11] in one of his synoptic papers. In his essay, the PWFS distinguishes itself in the wavefront sensors landscape for two main properties: (1) its ability to provide an accurate knowledge of the wavefront for different seeing conditions by varying its so-called modulation angle and (2) its enhanced sensitivity (at the expense of a reduced linearity between wavefront measurement and incoming phase signal) in closed loop operation[12] and beyond pupil spatial frequencies higher than the adopted modulation angle.[13] This is why today this sensor is a prime actor in AO systems design for the 30 m class telescopes and beyond.

However, so far, ray tracing of a pyramidal surface representing the PWFS has been addressed with different methods, but none of these fulfills the goal of a complete consistency with true PWFS layouts. These methods, in fact, address only some aspects of the propagation throughout a pyramidal optic, not the whole set, which limits the realm of applications of such kinds of modeling. For example, in the ray-tracing software ZEMAX™, a dioptric pyramidal surface is feasible exploiting four prismatic surfaces in the multiconfigurations mode, or using a unique nonsequential object mimicking the pyramidal surface itself. However, the multiconfiguration approach may be useful for the geometrical design. Instead, any attempt of a physical optical propagation will be meaningless in this case just because it is incompatible with the multiconfiguration tool. On the contrary, the use of a nonsequential object to define a pyramidal surface allows exploiting the physical propagation

*Address all correspondence to: Jacopo Antichi, E-mail: antichi@arcetri.inaf.it

2329-4124/2016/$25.00 © 2016 SPIE

Downloaded From: https://www.spiedigitallibrary.org/journals/Journal-of-Astronomical-Telescopes,-Instruments,-and-Systems on 14 Apr 2021
Terms of Use: https://www.spiedigitallibrary.org/terms-of-use

tool, which is useful to look, e.g., at the diffraction effects throughout a pyramidal optic. But it may become unphysical because a nonsequential surface is represented—generally in ray-tracing software—by a large number of discrete components. Depending on the adopted spatial sampling, the incoming beam may then not hit any of these, degrading the accuracy of the Fourier transforms used to retrieve the phase map along the optical path. Nevertheless, exploiting a nonsequential surface makes sensitivity analyses definitely complex and difficult to cross-check with true PWFS layouts, complicating the requirements analysis before the manufacturing of the final pyramidal optic, the core of this type of wavefront sensor.

To this aim, we have developed a user-defined dynamic link library (DLL) surface written in C, and working as the standard surface of the ray-tracing software ZEMAX™. The pyramid vertex and edges are accounted for in the code with explicit rules of propagation, and they are considered without any wideness just to perform the propagation through an ideal pyramidal surface. Consistency checks, based on ray-propagation statistics, certify that our recipe deals with the vertex and edges in a way compliant with refraction/reflection propagation rules once large numbers of rays are running in the ray-tracing software. This user-defined surface (UDS) DLL surface—named PAM2R, which stands for pyramidal acronyms may be too risky—is defined by an independent set of parameters explicit to the user. This method permits the user to both (1) manage the pyramidal surface during the ray-tracing modeling, allowing control of the whole set of dependent parameters and (2) lower error propagation, which is of benefit to any subsequent sensitivity analyses. We tested PAM2R to model the Giant Magellan Telescope (GMT) PWFS,[14] obtaining the required sensitivities for its pyramidal optics by ray-tracing software simulations only, as is possible for other standard optical surfaces in ZEMAX™.

2 Algorithms Defining Surface Rendering and Ray Tracing with PAM2R

Scalar quantities are set in lower case, no bold, and vector quantities in lower case, bold. Angular quantities are set with italic font, upper case, no bold. Symbol | is a scalar product, symbol × is a vector product, and the symbol | | is a vector modulus. The Euclidean space has its origin at the pyramid vertex **o**. The adopted coordinates reference frame has its origin at this point and follows a counterclockwise rotation rule. In this reference frame, a ray is defined by the following set of parameters:

- its position coordinates the $z = 0$ plane: $\mathbf{r}_0 = (x_0, y_0, 0)$,
- its direction cosines vector: $\mathbf{e} = [l, m, (1 - l^2 + m^2)^{1/2}]$, which in turn are linked to the ray field angles by the following relations: $\tan(\alpha) = l/n$; $\tan(\beta) = m/n$,
- the equation linking the position coordinates at the pyramid surface with the ones at the $z = 0$ plane: $\mathbf{r} = \mathbf{r}_0 + t\mathbf{e}$, where t is the distance between the position of the ray at the $z = 0$ plane and the position of the ray at the pyramidal optic surface.

2.1 *Pyramidal Surface Parameterization*

The surface parameterization lies upon the definition of the first face (see Fig. 1) by the following steps:

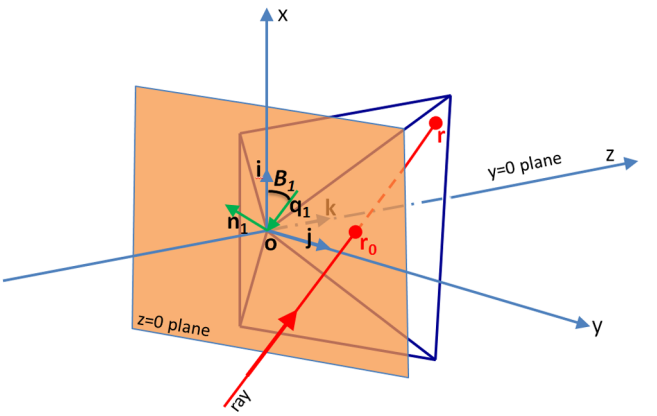

Fig. 1 Synopsis of the pyramidal surface parametrization.

1. rotation of $z = 0$ plane around the **−j** unitary vector of an angle B_1 within $(-\pi/2, \pi/2)$;
2. definition of the semiplane containing such face in the $x > 0$ subspace;
3. definition of the intersection line between this semiplane and the $y = 0$ plane, identified by the line unitary vector $\mathbf{q}_1$, which is oriented from the edge to the vertex of the pyramid;
4. rotation of the semiplane around unitary vector $\mathbf{q}_1$ of a tilt angle T_1 within $(-\pi/2, \pi/2)$.

Definitions of faces 2, 3, and 4 uses the same procedure of face 1 according to Table 1.

2.2 *Computation of the Unitary Vectors Shaping the Pyramidal Surface*

The equation of a plane lies on the unitary vector orthogonal to the plane (a.k.a. normal) and on a single point standing on the plane. We define **n** as the normal to a plane containing a face of the pyramidal surface. Referring to Fig. 1, it is easy to define the normal to face 1 as

$$\mathbf{n}_1 = [-\sin B_1, 0, \cos B_1], \tag{1}$$

and the line unitary vector $\mathbf{q}_1$ can be defined as

$$\mathbf{q}_1 = [-\cos B_1, 0, -\sin B_1]. \tag{2}$$

A rotation around $\mathbf{q}_1$ of an angle T_1 implies a modification of the components of $\mathbf{n}_1$ as

Table 1 Pyramidal surface faces definition.

Pyramid face number	Unitary vector rotation	Face subspace	Useful crossing plane	Line unitary vector
1	**−j**	$x > 0$	$y = 0$	$\mathbf{q}_1$
2	**+i**	$y > 0$	$x = 0$	$\mathbf{q}_2$
3	**+j**	$x < 0$	$y = 0$	$\mathbf{q}_3$
4	**−i**	$y < 0$	$x = 0$	$\mathbf{q}_4$

Downloaded From: https://www.spiedigitallibrary.org/journals/Journal-of-Astronomical-Telescopes,-Instruments,-and-Systems on 14 Apr 2021
Terms of Use: https://www.spiedigitallibrary.org/terms-of-use

$$\mathbf{n}_1 = [-\sin B_1 \cos T_1, \sin T_1, \cos B_1 \cos T_1], \tag{3}$$

and for the other faces, it turns

$$\begin{aligned}\mathbf{n}_2 &= [-\sin T_2, -\sin B_2 \cos T_2, \cos B_2 \cos T_2],\\ \mathbf{n}_3 &= [\sin B_3 \cos T_3, -\sin T_3, \cos B_3 \cos T_3],\\ \mathbf{n}_4 &= [\sin T_4, \sin B_4 \cos T_4, \cos B_4 \cos T_4].\end{aligned} \tag{4}$$

We name base angles set $[B_1, B_2, B_3, B_4]$ and tilt angles set $[T_1, T_2, T_3, T_4]$. Each component of the first set fixes the angle of each face with respect to the pyramid base, while each component of the second set fixes the orientation of each face with respect to its corresponding component of the tensor $[\mathbf{q}_1, \mathbf{q}_2, \mathbf{q}_3, \mathbf{q}_4]$.

2.3 *Computation of the Unitary Vectors Defining the Pyramid Surface Edges and Faces*

We define as an edge the intersection between the planes containing two faces. Hence, an edge is simultaneously orthogonal to the normal vectors of the two faces. This means that the edge line is along the direction defined by the vector product between the normal vectors of such faces. According to Fig. 2, face 1 is limited by the edge with face 4 on one side and the edge with face 2 to the other side. We then define $\mathbf{s}_A$ and $\mathbf{s}_B$ as the unitary vector of the edges limiting face 1 with the origin in the pyramidal surface vertex and direction toward the pyramidal surface base as

$$\mathbf{s}_A = \frac{\mathbf{n}_4 \times \mathbf{n}_1}{|\mathbf{n}_4 \times \mathbf{n}_1|}, \quad \mathbf{s}_B = \frac{\mathbf{n}_1 \times \mathbf{n}_2}{|\mathbf{n}_1 \times \mathbf{n}_2|}. \tag{5}$$

Equivalently, the remaining unitary vectors $\mathbf{s}_C$ and $\mathbf{s}_D$ can be written as

$$\mathbf{s}_C = \frac{\mathbf{n}_2 \times \mathbf{n}_3}{|\mathbf{n}_2 \times \mathbf{n}_3|}, \quad \mathbf{s}_D = \frac{\mathbf{n}_3 \times \mathbf{n}_4}{|\mathbf{n}_3 \times \mathbf{n}_4|}. \tag{6}$$

2.4 *Intersection Point of a Ray with a Face and Membership of this Point with Such Face*

The equation of a plane is defined by exploiting the vector orthogonal to such a plane and one point belonging to the plane. Thus, $\mathbf{n}_1$ being the normal to face 1, the equation of the plane containing face 1 is

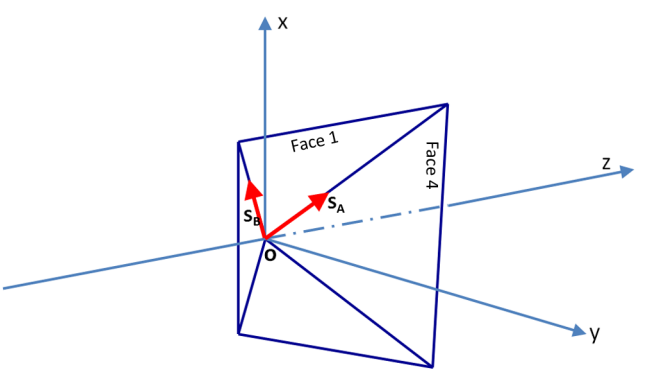

Fig. 2 Scheme useful to the definition of the edges' unitary vectors $\mathbf{s}_A$ and $\mathbf{s}_B$ for face 1.

$$\mathbf{r}|\mathbf{n}_1 = 0, \tag{7}$$

and combining this last one with the equation of the ray, we have

$$\mathbf{r} = \mathbf{r}_0 - \frac{\mathbf{r}_0|\mathbf{n}_1}{\mathbf{e}|\mathbf{n}_1}\mathbf{e}. \tag{8}$$

Equation (8) fixes the intersection point of the ray at the pyramidal surface as a function of input parameters. The computation of the direction cosines output from the pyramidal surface is finally achievable by applying Snell's refractive/reflective rule between each component of vector $\mathbf{e}$ and $\mathbf{n}_1$ at the intersection point $\mathbf{r}$. (Note that the above formalism is valid only when the ray and the plane containing the face are not parallel to each other.) Nevertheless, in the plane containing face 1, unitary vectors $\mathbf{s}_A$ and $\mathbf{s}_B$ form a nonorthogonal base proper to the bidimensional space affine to face 1 having an origin at $\mathbf{o}$.

Vector $\mathbf{r}$ can then be written as a linear combination of vectors $\mathbf{s}_A$ and $\mathbf{s}_B$ with position coordinates γ and δ as follows

$$\begin{aligned}\gamma &= \frac{\mathbf{r}|\mathbf{s}_A - (\mathbf{r}|\mathbf{s}_B)(\mathbf{s}_A|\mathbf{s}_B)}{1 - (\mathbf{s}_A|\mathbf{s}_B)^2},\\ \delta &= \frac{\mathbf{r}|\mathbf{s}_B - (\mathbf{r}|\mathbf{s}_A)(\mathbf{s}_A|\mathbf{s}_B)}{1 - (\mathbf{s}_A|\mathbf{s}_B)^2}.\end{aligned} \tag{9}$$

Hence, the intersection point of the ray belongs to the subspace corresponding to face 1, if and only if γ and δ are both positive. The same procedure applies to the other faces. This condition allows PAM2R to propagate rays within the pyramidal surface. Similar equations govern the intersection point between a ray and the other faces of the pyramidal surface.

Finally, as a general remark, it is important to stress that propagation throughout an optical system loading PAM2R is allowed only if this surface is defined after the position of the aperture stop. This is due to the need of ZEMAX™ to trace the field center chief ray, from object space to aperture stop center. In this respect, PAM2R is not different from any nonsequential component inserted within a sequential design obtained with this software.

3 Implementation of PAM2R in ZEMAX™ as User-Defined Surface Dynamic Link Library Surface

PAM2R is implemented as a UDS surface exploiting a DLL file developed from the mathematical approach described in Sec. 2 by using the coding conventions described in the ZEMAX™ manual, following the example file: `usersurface.c`. In detail, for each ray, which is defined by its direction cosines and position vectors at the $z = 0$ plane, PAM2R evaluates the position vector $\mathbf{r}$ on the pyramidal surface. Thus, the pyramidal surface base and tilt angles fix the pyramid geometry.

At the software graphical user interface (GUI), PAM2R exhibits its parameters both in the lens data editor (LDE) and in the extra data editor (EDE). In the LDE GUI, aside from typical parameters proper to the surfaces, PAM2R allows indicating the four base angles in degrees named: B1, B2, B3, and B4. In the EDE GUI, height extra parameters permit to further customize the pyramidal surface: dB1, dB2, dB3, dB4, dT1, dT2, dT3, dT4. PAM2R independently operates on each element of both base angles and tilt angles sets. Specifically, from angle dB1 to angle dB4, PAM2R allows introducing errors on the pyramid

Downloaded From: https://www.spiedigitallibrary.org/journals/Journal-of-Astronomical-Telescopes,-Instruments,-and-Systems on 14 Apr 2021
Terms of Use: https://www.spiedigitallibrary.org/terms-of-use

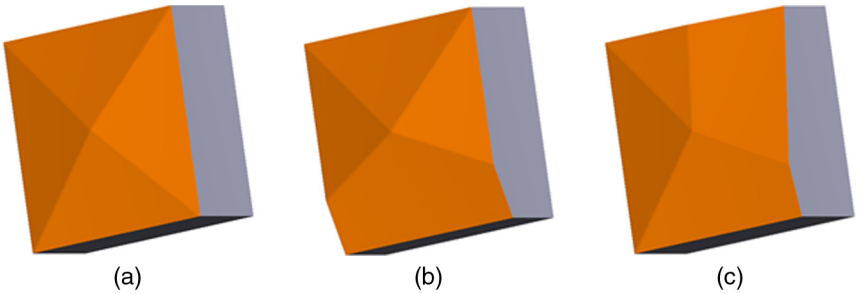

Fig. 3 (a) Perfect pyramidal surface; (b) imperfect pyramidal surface showing 10 deg error of the base angle on its lower face; (c) imperfect pyramidal surface showing 10 deg error of the tilt angle on its right face.

base angles set, letting their actual values become B1 + dB1, B2 + dB2, B3 + dB3, and B4 + dB4. Figure 3 shows a setting for base angle deviations from nominal values in degree units, which is as follows: $[\mathrm{dB1}, \mathrm{dB2}, \mathrm{dB3}, \mathrm{dB4}] = [0,0,10,0]$. Four further parameters—dT1, dT2, dT3, and dT4—fix the variation of the tilt angles, whose referring values T1, T2, T3, and T4 are set equal to 0. The same figure shows a setting for tilt angle deviations from nominal values in degree units, which is as follows: $[\mathrm{dT1}, \mathrm{dT2}, \mathrm{dT3}, \mathrm{dT4}] = [0,0,0,10]$.

PAM2R has been tested on Radiant ZEMAX™ 13 Release 2 SP6 Professional and on Radiant OpticStudio™ 15.5 Professional, both for 64 bit WINDOWS™ platforms. Details can be found in Ref. 15.

4 Sensitivity Analysis of the Pyramid Wavefront Sensor Baseline Design for the Giant Magellan Telescope Adaptive Optics System with PAM2R

The GMT is a 25.4-m-diameter ground-based telescope having a Gregorian optical design. Its primary mirror is composed of seven monolithic mirrors 8.4-m-diameter wide, and shaped on a hexagonal lattice. Currently under construction on Cerro Las Campanas in northern Chile, GMT is one of the world's few extremely large telescopes of the next decade. Its AO system will provide three observing modes using different wavefront sensing approaches to balance turbulence compensation with sky coverage and field of view.[16] Specifically, its single-conjugated natural guide star AO system is a complex PWFS layout made of two distinct channels. The first (fast tracking sensor) is aimed at the adaptive compensation of the atmospheric turbulence and the residual dynamical telescopes aberrations. The second (slow tracking sensor) is aimed at the compensation of the relative piston among primary mirror segments.[14] As shown in Fig. 4, both the fast tracking wavefront sensor (after reflection with the beam splitter first surface) and slow tracking wavefront sensor (after transmission through the beam splitter) are identical and shaped with a double-glass pyramidal optic. A sensitivity analysis of the whole set of shaping angles of the two GMT PWFS pyramidal optics was considered essential during the design phase in order to fix all the required angular constraints before production of any witness sample. In general, sensitivity analysis is important to define a production strategy respecting a given error budget. Thus, the error budget establishes the main constraints the lens maker should respect before realizing the final product, matching the required specifications. To this aim, the main term of the error budget for a PWFS lies upon the variation of the distance

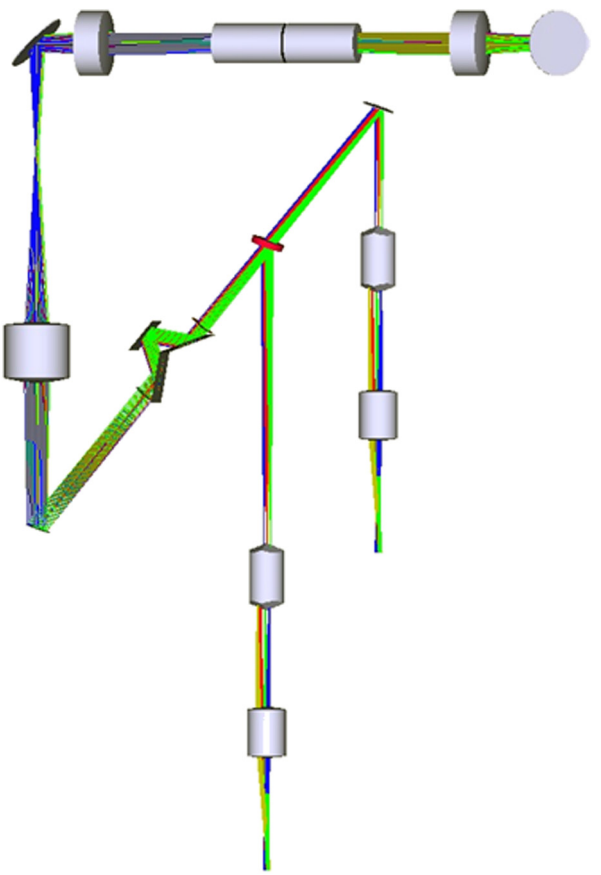

Fig. 4 Rendering of the GMT natural guide star PWFS system. Colors are field of views. The input beam starts top-right from a pick-up mirror which bends the beam inside the atmospheric diffraction compensator module shown at top-center. This optical element works within a collimated beam, provided by a suitable lens adopted as collimator. Telecentricity downstream is restored by using such lens inversely. Telecentricity in turn is essential, for FLAO-like PWFS designs, to let the AO bench selecting its reference star through rigid movements only and provided by a dual-axis mechanical stage screwed to the bench at its bottom. Another pick-up mirror bends the beam toward a focusing lens, providing two distinct focus at the vertex of a couple of double-glass pyramidal optic, separated by a beam-splitter shown by a red color. This optics divides the fast tracking wavefront sensor to the slow tracking wavefront sensor. The fast tracking wavefront sensor receives reflected light from the beam splitter, while the slow tracking wavefront sensor receives light in transmission from the beam splitter. The *K*-shaped catoptric unit before the beam splitter allows restoring the pupil-stabilized mode, which in turn is essential for AO. These two PWFS have a double-glass pyramidal optic with the first surface base angles all equal 30.000 deg and the second surface base angles all equal 28.384 deg.

Downloaded From: https://www.spiedigitallibrary.org/journals/Journal-of-Astronomical-Telescopes,-Instruments,-and-Systems on 14 Apr 2021
Terms of Use: https://www.spiedigitallibrary.org/terms-of-use

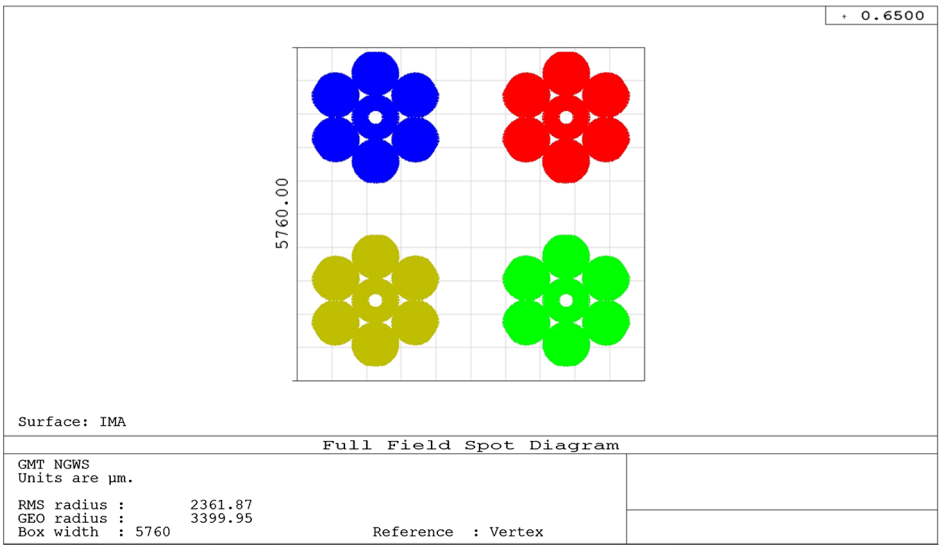

Fig. 5 Four pupils reimaging at the GMT PWFS image plane. Pupils shape respects the one of the GMT entrance pupil shape. The square side is in microns and corresponds to 240 pixels (with size equals 0.024 mm). Pupils have linear size equal to 92 pixels and distance between centers equal to 132 pixels side.

among reimaged pupils' centers, which in turn depends directly on the pyramidal optics constructive angles.

Thanks to the experience achieved with the FLAO PWFS, the control loop performance degradation induced by a pupil shift smaller than 0.1 subaperture has been recognized to be not significant. This requirement has been adopted during the GMT PWFS simulations also, confirming that good control loop performances are achievable for this AO system as well. In terms of AO sampling, this performance requirement corresponds to a pupil shift that equals 0.11% of the GMT telescope one. If no rebinning is applied to the wavefront sensor pupils' image, this requirement corresponds to 0.1 detector pixel. With this number in mind, a detailed tolerance analysis has been made for this glass pyramidal optic, highlighting sensitivities with respect to its constructive errors: (1) base angle per pyramid face, (2) tilt angle per pyramid face, (3) maximum wedge angle error between adjacent pyramidal optics, (4) maximum coregistration error between adjacent pyramidal optics, and (5) maximum variations of refraction index and Abbe number for the glasses (N-SK11 and N-PSK53A) shaping this double-glass pyramidal optic. Sensitivities obtained were as follows: (1) 0.202 micron/arc sec, (2) 0.172 micron/arc sec, (3) 0.0463 micron/arc sec, (4) 15 micron/mm, and (5) refraction index and Abbe number precisions equal to 0.0002 and 0.003, respectively. These sensitivities have been broken down into an error budget, sorting out the maximum base and tilt

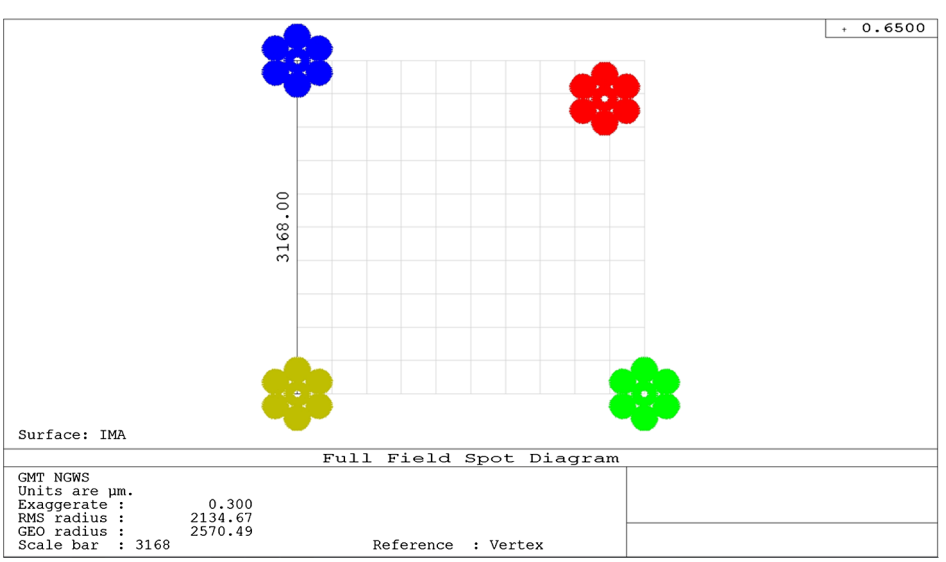

Fig. 6 Example of a manufacturing error (0.5 deg) of one of the four base angles proper to the first pyramidal surface shaping the GMT PWFS and acting on the top-right (red color) pupil. The square side is in microns and corresponds to 132 pixels. Reimaged pupils setup is the same of Fig. 5.

Downloaded From: https://www.spiedigitallibrary.org/journals/Journal-of-Astronomical-Telescopes,-Instruments,-and-Systems on 14 Apr 2021
Terms of Use: https://www.spiedigitallibrary.org/terms-of-use

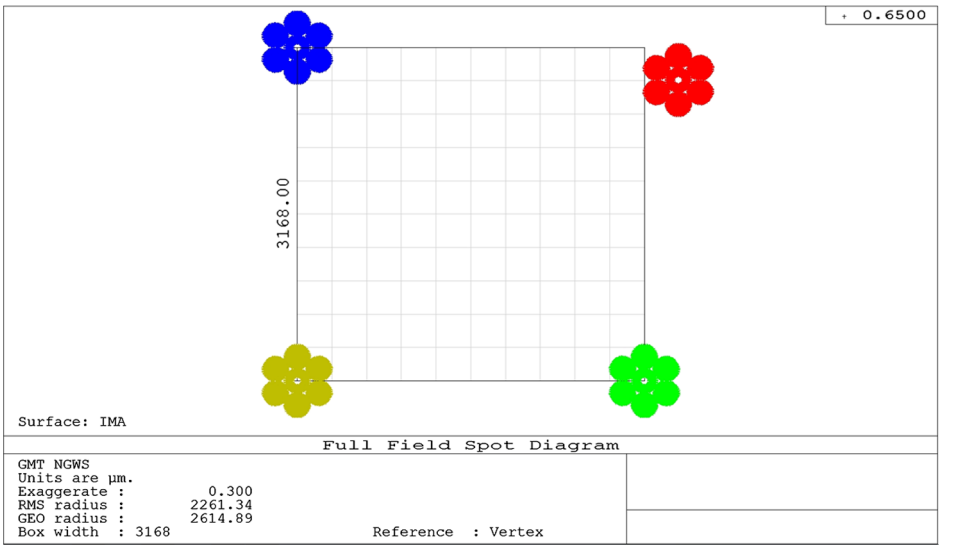

Fig. 7 Example of a manufacturing error (0.5 deg) of one of the four tilt angles proper to the first pyramidal surface shaping the GMT PWFS and acting on the top-right pupil (red color). The square side is in microns and corresponds to 132 pixels. Reimaged pupils setup is the same of Fig. 5.

angles' error, per pyramid face, matching the global performance requirement of 0.1 subaperture maximum pupil shift. This value returns 2 arc sec (5.6×10^{-4} deg) both for base and tilt angles, per pyramid face. Though this angular constructive specification is challenging, it depends on the nominal values selected for the base angles of this kind of optic. Aware of this, the nominal base angles of the GMT PWFS have been selected to be as close as possible to the ones of the FLAO PWFS, whose as-built optics has been manufactured and polished with standard techniques.

The corresponding performance degradation of the pupil shift position is presented by Figs. 5–7, where the ideal case, the maximum tolerated base angle, and the maximum tolerated tilt angle cases are shown in this order. PAM2R allows this kind of sensitivity analysis just because both base and tilt angles, together with the thickness and the glass type, form the independent set of parameters defining each single sequential pyramidal surface in ZEMAX™. In this way, angular constructive tolerances are achievable by ray tracing only.

5 Conclusions

This paper describes a user-defined DLL surface named PAM2R. Its source code is procedural and written in C. Its output is the optical beam propagation throughout a pyramidal surface. We exploited PAM2R to (1) design the GTM AO PWFS system and (2) obtain the required sensitivities for the constructive angles of its pyramidal optics, hence demonstrating its reliability and robustness. PAM2R represents the tool to design PWFSs, as is commonly done for other wavefront sensor types. This will benefit AO system designs, especially in the case of extremely large telescopes, where this sensor is expected to be highly competitive.[17,18]

Acknowledgments

The authors would like to thank Andrew Rakich, Célia Protin-Blain, Gianluca Di Rico, Peter Wizinowich, and Jess Koehler for their fruitful remarks to the paper.

References

1. R. Ragazzoni, "Pupil plane wavefront sensing with an oscillating prism," *J. Mod. Opt.* **43**, 289–293 (1996).
2. E. Diolaiti et al., "Some novel concept in multipyramid wavefront sensing," *Proc. SPIE* **4839**, 299–306 (2003).
3. A. Tozzi et al., "The double pyramid wavefront sensor for LBT," *Proc. SPIE* **7015**, 701558 (2008).
4. A. Wang et al., "Design and fabrication of a pyramid wavefront sensor," *Opt. Eng.* **49**(7), 073401 (2010).
5. R. Ragazzoni et al., "The pyramid wavefront sensor aboard Adopt@TNG and beyond: a status report," *Proc. SPIE* **4494**, 181–187 (2002).
6. E. Marchetti et al., "MAD the ESO multi-conjugate adaptive optics demonstrator," *Proc. SPIE* **4839**, 317–328 (2003).
7. S. Esposito et al., "First light adaptive optics system for large binocular telescope," *Proc. SPIE* **4839**, 164–173 (2003).
8. K. M. Morzinsky et al., "MagAO: status and on-sky performance of the Magellan adaptive optics system," *Proc. SPIE* **9148**, 914804 (2014).
9. N. Jovanovic et al., "The subaru coronagraphic extreme adaptive optics system: enabling high-contrast imaging on solar-system scales," *Publ. Astron. Soc. Pac.* **127**, 890–910 (2015).
10. A. Riccardi et al., "The NGS pyramid wavefront sensor for ERIS," *Proc. SPIE* **9148**, 91483D (2014).
11. O. Guyon, "Limits of adaptive optics for high-contrast imaging," *Astrophys. J.* **629**, 592–614 (2005).
12. R. Ragazzoni and J. Farinato, "Sensitivity of a pyramidic wave front sensor in closed loop adaptive optics," *Astron. Astrophys.* **350**, L23–L26 (1999).
13. C. Vérinaud, "On the nature of the measurements provided by a pyramid wave-front sensor," *Opt. Commun.* **233**, 27–38 (2004).
14. E. Pinna et al., "Design and numerical simulations of the GMT Natural Guide star WFS," *Proc. SPIE* **9148**, 91482M (2014).
15. M. Munari et al., "PAM2R," 2016, http://pam2r.arcetri.astro.it/ (13 May 2016).
16. A. H. Bouchez et al., "The Giant Magellan telescope adaptive optics program," *Proc. SPIE* **8447**, 84471I (2012).
17. C. Vérinaud et al., "Adaptive optics for high-contrast imaging: pyramid sensor versus spatially filtered Shack–Hartmann sensor," *Mon. Not. R. Astron. Soc. Lett.* **357**, L26–L30 (2005).
18. A. Carlotti et al., "Modelization of a pyramid wavefront sensor for the E-ELT in the context of the COMPASS project," *Proc. SPIE* **9148**, 91486R (2014).

Jacopo Antichi received his laurea degree in physics, his MSc in applied optics, and his PhD in astronomy at the Università degli

Downloaded From: https://www.spiedigitallibrary.org/journals/Journal-of-Astronomical-Telescopes,-Instruments,-and-Systems on 14 Apr 2021
Terms of Use: https://www.spiedigitallibrary.org/terms-of-use

Studi di Padova in 2002, 2003, and 2007, respectively. His interests include exoplanet imaging with integral field spectroscopy and interferometry supported by adaptive optics. Since 2012, he is a senior scientist fellow at INAF-Arcetri Astrophysical Observatory.

Matteo Munari received his laurea in physics at the Università degli Studi di Padova in 2005. He has worked at INAF-Catania Astrophysical Observatory since 2007, starting in 2012 as a staff researcher. He is interested in ground- and space-based optical system designs, solar physics instruments, and exoplanet imaging.

Demetrio Magrin received his laurea degree in physics in 2001 and his PhD in astronomy in 2006, both at the Università degli Studi di Padova. He has been a staff researcher at INAF-Padova Astronomical Observatory since 2012. His interests include ground- and space-based optical system designs, adaptive optics systems, and exoplanet imaging.

Armando Riccardi received his laurea degree in physics in 1996 on a pyramid wavefront sensor development at the Università degli Studi di Firenze. He is a staff researcher at INAF-Arcetri Astrophysical Observatory since 2002. His field of research is adaptive optics for astronomy, in particular the development of large-format deformable mirrors and wavefront sensors.

Downloaded From: https://www.spiedigitallibrary.org/journals/Journal-of-Astronomical-Telescopes,-Instruments,-and-Systems on 14 Apr 2021
Terms of Use: https://www.spiedigitallibrary.org/terms-of-use